



Combustion system optimization for the integration of e-fuels (Oxymethylene Ether) in compression ignition engines

Ricardo Novella, Gabriela Bracho^{*}, Josep Gomez-Soriano, Cássio S. Fernandes, Tommaso Lucchini

CMT – Motores Térmicos, Universitat Politècnica de València, Spain
Politecnico di Milano, Italy

ARTICLE INFO

Keywords:

Internal combustion engines
CFD codes
Optimization algorithm
Alternative fuel
OME

ABSTRACT

In this study, a numerical methodology for the optimization of the combustion chamber in compression ignited engines using OME as fuel is presented. The objective is to obtain a dedicated combustion system for an engine that is fueled with this alternative fuel improving the efficiency and reducing the emissions of NO_x. This article proposes the integration between the optimization algorithm and CFD codes to evaluate the behavior of an engine fuelled with the low sooting fuel OME. Based on a diesel model validated against experimental data, a further model for OME fuel was implemented for evaluating the performance of the engine. The particle swarm algorithm (PSO) was modified based on the Novelty Search concepts and used as optimization algorithm. Several tools are coupled in order to create each CFD case where all the tools and optimization algorithm are coupled in a routine that automates the entire process. The result is an optimized combustion system that provides an increase of the efficiency (about 2.2%) and a NO_x reduction (35.7%) in comparison with the baseline engine with conventional fuel. In addition, a neuronal network was trained with all the results of all simulations performed during the optimization process, studying the influence of each parameter on the emissions and efficiency. From this analysis it was concluded that the EGR rate and injection pressure affects the NO_x emissions with a range of variability of 63% and 38% respectively.

1. Introduction

Modern society is in continuous search of solutions for reducing Greenhouse Gases (GHG) emissions, especially in the industrial and transport sectors, in a sustainable way. These two sectors contributed in about 75 % of CO₂ emissions in the last decade as appraised in a recent works [1]. To control these emissions, strict regulations have been established promoting great effort in research and in the industry fields, where new technologies and systems are being developed, such as the implementation of electrified powertrains and the utilization of different fuels as hydrogen or with low carbon content [2].

An alternative for reducing GHG emissions is to replace conventional propellant by synthetic fuels from renewable sources. Among the various renewable fuels, the Oxymethylene Ethers (OMEs) have gained attention since they produce lower levels of particulate matter (PM) and Carbon Oxide (CO) emissions as is reported in previous studies [3–8]. The production of OME starts from methanol, where methanol is

produced by the reaction of H₂ and CO₂ [9,10].

OMEs are liquid fuels that can be used in substitution or as blend with conventional diesel fuel using engine architectures that are available in the market nowadays with minor modifications. In comparison with conventional diesel, OME contains a high quantity of oxygen, which avoids soot emission production during the combustion process [6,11]. Due to this higher oxygen content it is possible to work with a high EGR level being possible to reduce Nitrous Oxides (NO_x) emissions as well [12]. However, other difference with respect to conventional fuel is that they have a lower heating value, which has to be compensated with longer injections, higher rail pressures or nozzles with larger diameters if an equivalent energy release to that of a traditional fossil fuel is required [13]. Most of previous studies done with these fuels have been carried out for pre-existing conventional engine architectures, however recent studies report that the performance could be further improved by adapting the combustion system configuration to the chemical requirements of this renewable fuel. In this regard, Gaukel

^{*} Corresponding author.

E-mail address: gbracho@mot.upv.es (G. Bracho).

<https://doi.org/10.1016/j.fuel.2021.121580>

Received 7 April 2021; Received in revised form 29 June 2021; Accepted 26 July 2021

Available online 5 August 2021

0016-2361/© 2021 Elsevier Ltd. All rights reserved.

et al. [14] reported an experimental and computational study on an engine fueled with OME, where they tested 10 different piston bowl shape configurations. From all the bowl piston configurations that were evaluated, they found a combination that reduced the NO_x emissions and maintained the indicated efficiency at the same time. They concluded that the piston design has a strong influence on the combustion performance, and recommended further research to explore other geometries, combined with different injection and EGR strategies, simultaneously. It is possible to perform multivariate studies experimentally but it is expensive and requires many hours in the test-bench. A common approach, is to combine the experimental activities with the use of Computational Fluid Dynamics (CFD) tools in the design process of the combustion systems. Once the model is validated with experimental data, it is possible to generate different engine configurations and to test them computationally at an affordable time and cost [15]. Furthermore, the use of computer-aided methodologies will help not only to reduce the costs of engine development but also to redirect efforts to optimize other industrial procedures derived from its development, contributing to reduce the environmental footprint of all involved activities.

In the analysis of the combustion process for a system configuration, designers should take into account that combustion itself is a complex phenomenon due to the high dependence of several parameters, which are generally non-linear and with cross-interaction between them. Finding the right combination of all the factors that provides an optimal engine design is a challenge nowadays. As an alternative, different algorithms for optimization as Genetic Algorithm (GA), Particle Swarm Optimization (PSO), or combinations between them are used in recent engines design works.

Braatch et al. in [15] presented an approach that combines CFD modeling with GA to optimize the combustion system of a compression ignited engine fueled with conventional diesel, reducing both fuel consumption and combustion noise. They selected eight variables related to piston bowl geometry, nozzle angle, number of injector nozzle holes and in-cylinder swirl motion intensity. After seven hundreds simulations approximately they found an optimum configuration that showed a lower combustion noise and improved efficiency compared to the baseline system, and within the limits of soot and NO_x emissions. Another optimization process was proposed by Bertram et al. in [16], based on a hybrid method between GA and PSO for optimizing a conventional diesel engine performance. Results show the benefits and weaknesses of both algorithms. They reported that the enhanced hybrid approach offered a faster convergence because of the PSO aggressive acceleration towards the best case.

Concerning optimization procedures for alternative low sooting fuels from renewable sources like Dimethyl Ethet (DME) or OMEs, few recent studies can be found. Zubel et al. in [17] performed an investigation using GA to optimize the piston bowl shape and injector nozzle geometry of an engine fuelled with DME. Since the lower heating value of DME is lower than the diesel value, new larger nozzle holes were proposed. Their numerical optimization predicted an improvement on efficiency and a reduction of HC and CO emissions simultaneously. Although they found promising results, they also suggested to include more parameters on the evaluation of the system such as the swirl level. Based on their conclusions, it can be deduced that more efforts can be done in this regard to maximize the benefits of these promising fuels.

The aim of this work is to provide the best combustion system design for the integration of OME fuel in a compression ignited engine using a novel optimization methodology. Part of this study consists on developing a computational fluid dynamics engine model with detailed chemistry, at full load operating condition in a traditional engine architecture. Once the model is validated, it is included in a PSO optimization algorithm, where 12 parameters are evaluated simultaneously, such as piston geometry (defined by 6 control points), number of injector nozzles, included spray angle, swirl number, injection pressure, EGR rate and pressure at the intake valve closing (IVC), therefore

adapting the geometry characteristics of the combustion chamber to the requirements of this renewable fuel. The target during the optimization will be to maximize the engine efficiency while decreasing NO_x emissions, taking advantage of the low sooting nature of this fuel.

The article is structured as follows. Section 2 describes the fuel characteristics and properties. Section 3 presents all the tools and methodology used in this work. In this section the engine configuration, computational approach, CFD models and its validation, optimization algorithm and tools are described. In the Section 4 the obtained results are presented and discussed. Section 5 presents a parametric study performed with a neuronal network methodology to evaluate the optimized case. Finally, Section 5 present the conclusions of the work.

2. Investigated fuel characteristics

In this study Oxymethyl Ether (OME) is used, which is a fuel that produces an almost soot free combustion, even at stoichiometric air/fuel conditions. Among other oxygenates, OME seems to be convenient in engine application since its general physico-chemical properties are relatively similar to conventional diesel, not requiring major modifications. However, as well as other oxygenated compounds, OME has some different properties in comparison to conventional diesel (viscosity, density, lower heating value). The key properties of the fuels used in this study are listed in the Table 1.

In particular, the lower heating value (LHV) of OME needs to be compensated to obtain the same amount of released energy during the combustion compared to the one obtained with diesel fuel. Different strategies can be employed for compensating this decrease in LHV. One of them is to extend the duration of the injection in order to deliver more fuel mass amount into the combustion chamber, but this results in a decrease of the combustion efficiency because part of the combustion occurs late. A second possibility could be to increase the rail pressure in order to deliver a higher mass flow rate, keeping the injection duration short enough. However, this strategy might have an effect on the spray structure and on the wall impingement, together with the limitation on the maximum pressure that the pump system can supply. The third option is to increase the total area of the nozzle, either by increasing the hole number, scaling the hole diameter, or both simultaneously. For this option the limitation is on the maximum hole number due to manufacturing and material constrains. For this investigation a combination of the total area scaling is considered in the design of the system during the optimization process. The scaling factor for the same energy flow rate of OME and Diesel is determined by Eqs. (1) and (2) based on the energy available in the fuel and the Bernoulli's principle for incompressible flows (assuming that the velocity of the flow would be similar when the pressure difference is the same).

$$\dot{m}_{ome} \cdot LHV_{ome} = \dot{m}_d \cdot LHV_d \quad (1)$$

$$A_{ome} \cdot \rho_{ome} \cdot u \cdot LHV_{ome} = A_d \cdot \rho_d \cdot u \cdot LHV_d, \quad (2)$$

where A is the total area of the nozzle, LHV is the lower heating value, ρ the density of the fuel, and u the flow velocity in the nozzle exit. The subscripts *ome* and *d* denote OME and diesel fuel respectively. The total area is defined as Eq. (3), being *n* the number of holes and *d_o* the exit hole diameter.

Table 1
Physical and chemical properties of the fuel.

Fuel	OME	Diesel
Density (15°C [kg/m ³])	860	830
Viscosity (40°C [mm ² /s])	1.18	≈3
Oxygen content [wt%]	42.1 [4]	≈0
LHV [MJ/kg]	22.4	43
Boiling point [°C]	42	180–350

$$A = \frac{n \cdot \pi \cdot d_o^2}{4} \quad (3)$$

3. Tools and methodology

In this section, the methodology and the tools are presented in detail. The sequence of the description corresponds to the workflow followed during the study, and it is divided in two blocks. The first block is related to the development of the CFD model and validation of the reference engine, where data from an experimental engine was used. Later on, in the same block, an explanation of the model configuration for OME fuel and preliminary results are shown. Afterwards, the second block details the mathematical approach used for the optimisation process which is based on the PSO algorithm, where all the additional tools programmed for an automatic process are also explained.

3.1. Engine configuration

The engine used is a medium-duty diesel engine for goods transportation. The tests were carried out in an experimental facility available at the laboratories of CMT Motores Termicos. It is a four-cylinder diesel engine with a compression ratio (CR) of 16, equipped with a turbocharger and a common-rail injection system. The operating conditions reproduced in the CFD model are representative of max power, running the engine at 3750 rpm and 18 bar of IMEP. The injection system is a common rail system with a ten-hole injector with diameter of 112 μm and an included spray angle of 154°. The engine specifications are summarized in Table 2. The simulations were performed in a closed cycle, it means from the instant of intake valve closing (IVC) until exhaust valve opening (EVO) involving the piston motion and a volume variation during the simulation. The parameters considered for the boundary conditions at IVC are the gas pressure and temperature, initial gas concentration, all wall temperatures and the injection settings (mass flow, rail pressure, start of injection).

3.2. Computational approach

For the combustion system simulation the Lib-ICE code was used, which is on the basis of OpenFOAM® technology [18], and includes a set of libraries and solvers for internal combustion engine simulations. Due to the high number of simulations that are done in the optimization stage, a robust model with enough performance in terms of computational time is required. For this reason, the domain is simplified based on the axy-symmetry of the combustion chamber, defining a sector of the geometry that is a function of the number of orifices of the injector nozzle. For the reference case the sector was 1/10 of the geometry. The piston movement is considered and is reproduced by the dynamic mesh layering technique available in Lib-ICE [19,20]. As the combustion process depends of physical and chemical phenomena several sub-models were used to reproduce correctly each phenomena during the CFD engine simulation.

Two different fuels were tested: N-heptane was used as diesel surrogate in the initial CFD model that was used as a reference and for validation against experimental data. The second one was OME, that was also employed in the engine optimization. For both fuels, the liquid

spray was simulated using a Lagrangian particle tracking model, assuming a “Blob” injection method [20,21]. The spray field and behavior inside the combustion chamber was created by grouping liquid droplets into parcels that can represent statistically the spray from a specific rate of injection (ROI) profile from a virtual injector model [22]. To reproduce the liquid atomization, heat transfer, break-up and evaporation, both, Kelvin–Helmholtz (KH) and Rayleigh–Taylor (RT) algorithms were used for the secondary break-up process [23,24]. The in-cylinder turbulence used in all simulation was modeled by Reynolds-Averaged Navier Stokes (RANS) based in re-normalized group (RNG $k-\epsilon$) [25]. To calculate the heat transfer Angelberger model was used coupled with the turbulence model. To reproduce the chemistry of the fuels two different chemical kinetic mechanism were implemented, for N-heptane the reduced mechanism containing 162 species and 1543 reactions and for OME it is composed by 534 species and 2901 reactions.

For the combustion and emissions predictions the Multi Representative Interactive Flamelet (mRIF) model approach was used, which is available in the Lib-ICE code. The model configures the flames structures as a set of unsteady diffusion flames that represents diesel combustion. The reaction–diffusion equations are solved in the mixture fraction space where species and energy equations are solved and the turbulence–chemistry interaction is governed by the scalar dissipation rate. Also, it is possible to predict the flame stabilization. The model development and validation is available in [26–30]. The models and sub-models used in this study are listed in Table 3.

3.3. Validation of the model

The CFD model was validated using data from an engine fueled with diesel, running at 3750 rpm and full power conditions. All the boundary conditions used in the model were obtained from the experimental data using an in-house methodology developed by Benajes et al. in [31]. The values are summarized in Table 4.

Different mesh configurations were appraised, to evaluate their impact on computational time and accuracy of the results. For instance, an initial simulation was performed with a well refined mesh in order to fit the experimental results with good accuracy. Later on, the mesh was coarsened until reaching a point that provides a better compromise between results precision and computational time. Both meshes, the fine and coarse mesh, can be seen in Fig. 1. The fine mesh counts with 52000 cells at TDC and the coarse mesh counts with 26900 and cells at TDC.

The comparison between in-cylinder pressure and heat release rate (HRR) results of experimental data against simulation results are shown in Fig. 2. In this figure the black, blue and red lines represent the experimental data, fine mesh and coarse mesh results respectively. Analyzing the results, the CFD predictions provide good agreement between experimental and simulations for both fine and coarse mesh. Moreover, with the fine mesh it is possible to obtain a better prediction between experiment and simulation but costs more in terms of a computational time. The coarse mesh presents minor differences respect to the fine mesh, but with lower computational time. Taking into account that for the optimization stage a large number of simulations are required, the coarse mesh was chosen as baseline mesh for all upcoming simulations, also this is used as the reference for further comparisons.

The next step consists of evaluating the performance of the engine

Table 2
Engine specifications.

Number of cylinders [–]	4
Volume [l]	2.2
Bore - stroke [mm]	85–96
Compression ratio [–]	16:1
Injector number of holes	10
Injector total area [m^2]	9.85e-06
Spray angle [deg]	154
Engine speed [rpm]	3750

Table 3
Models specifications.

Injection	Blob Injector
Break-up	KH-RT
Collision	off
Evaporation	standard
Turbulence	RNG $k-\epsilon$ RANS
Wall Heat transfer	Angelberger
Combustion	RIF
Soot	Leung Lindstedt Jones

Table 4
Boundary conditions.

IVC [deg]	-112
EVO [deg]	116
Number of injections [-]	1
SOI [deg]	-11
Injection pressure [bar]	1800
Temperature at IVC [K]	470
Pressure at IVC [bar]	3.89

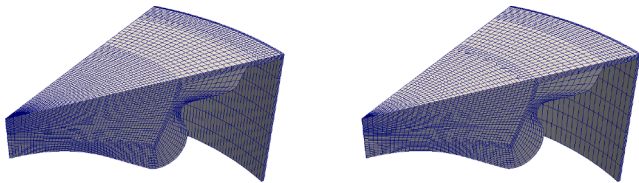


Fig. 1. Mesh comparison between fine mesh (left side) and coarse mesh (right side).

when OME is used as a fuel. The engine configuration in terms of boundary conditions were maintained equal than the baseline case. Though, all physical and chemical properties related to the fuel are updated accordingly, as well as the amount of fuel. The quantity of OME injected in the combustion chamber is adjusted to reach an equivalent amount of energy, since OME has a lower LHV than conventional diesel as was commented in Section 2. Fig. 3 shows the results obtained from the case running with OME against the diesel model previously calibrated. Analyzing the heat release rate traces it is confirmed that the mass fuel adjusted provides a similar quantity of energy released. The pressure trace when OME fuel is injected is slightly higher, but still below the limit of 180 bar recommended by the manufacturer to preserve the structural integrity of the cylinder. The heat release rate traces are comparable in terms of ignition delay, however, in the combustion diffusion phase OME presents a faster combustion and shows a short burn out phase, related to the higher volume of injected fuel. Regarding

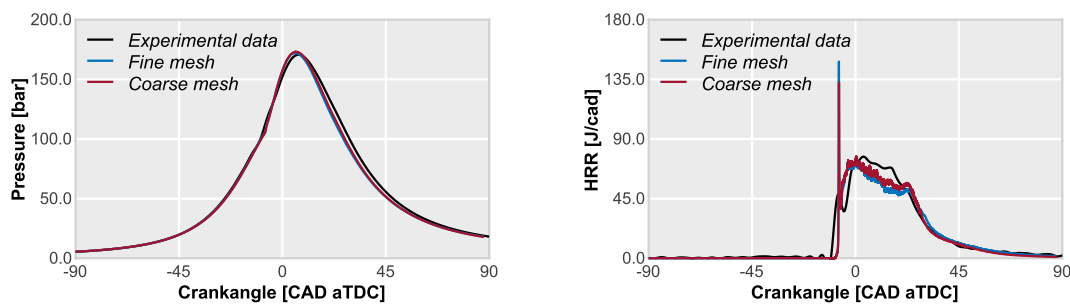


Fig. 2. Comparison between experimental data (black curve) and simulation results for fine and coarse meshes (blue and red curves respectively). Left side: Evolution of the in-cylinder pressure. Right side: Estimated Heat Release Rate. (For interpretation of the references to color in this figure legend, the reader is referred to the web version of this article.)

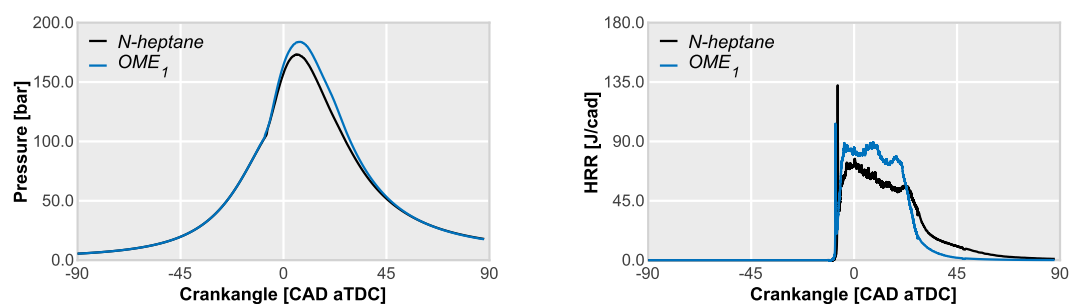


Fig. 3. Comparison between conventional diesel and OME fuel. Left side: Evolution of the in-cylinder pressure. Right side: Estimated Heat Release Rate.

the pollutant emissions, Table 5 shows the predicted results of soot and NO_x . As expected, soot emissions almost disappear when the engine is fueled with OME, although the NO_x levels are more than double than the diesel reference case. From this initial analysis it can be seen that the combustion with OME has an acceptable performance when it is used in a traditional architecture for a conventional fuel. Nevertheless, it seems that there is room for improvement if the combustion system is adapted to the OME fuel requirements by means of the optimization procedure.

3.4. Details of the computational optimization

To perform the optimization of the engine the Particle Swarm Optimization (PSO) algorithm was used. This algorithm was first proposed by Kennedy and Eberhart [32] and it is inspired in the behavior of birds flocking. Some advantages of the PSO include a fast rate of the convergence in the optimal solution, simple implementation, low cost to evaluate an objective function and can be applied in problems with a large parameters search spaces of candidates solutions. However, a few drawbacks of the algorithm are that it is not guaranteed that the optimal solution will be found because that the PSO can be stuck in a local minimum and the algorithm has a strong sensitivity to meta-parameters values [16]. During the execution of the algorithm search for the optimal, the PSO just requires a little information about position x_i update according the expression:

$$x_i(t+1) = x_i(t) + v_i(t+1), \quad (4)$$

and, the velocity is updated of each particle according the expression:

Table 5
Pollutant emissions results – Baseline Diesel and OME fuel.

Fuel	NO_x [mg/s]	Soot [mg/s]
Diesel	230.9	0.354
OME	773.6	1e-14

$$v_i(t+1) = w \beta \cdot v_i(t) + c_1 \tau \cdot (p_i - x_i(t)) + c_2 \gamma \cdot (g - x_i(t)), \quad (5)$$

where, t means the iteration, w is the inertia weight, c_1 and c_2 are the individual weight and social weight respectively referred to the individual factor. Generally the values used for w , c_1 and c_2 depend on the problem. The usual value for w is in the range of [0.5,1.5] and the coefficients c_1 and c_2 are in the range of [1,3]. The p_i represents the current best position of x_i and g is the global best position of all particles. The unknowns β , τ and γ are random vectors where each element of the vector is random of a uniform distribution in the range [0,1].

As already explained, the PSO algorithm has some drawbacks. Thus, seeking to improve the convergence issues in the PSO, an additional approach is implemented in the algorithm routine. In [33] the use of Novelty Search concepts is proposed to improve the exploration of the search space and, based in these concepts the generated particles are divided in, a first family, formed by “conquerors” particles and ruled by Eq. (1) as in the regular PSO and, the second family, formed by “explorers” particles where the Novelty Search (NS) concept is used. The names of conquerors and explorers particles are defined by their function in the algorithm, that is “to conquer” the optimum solution and the close regions and the “explorers” means that these particles must “explore” all the search space, even the regions that provide bad results. This approach aims to avoid that the PSO be stuck in a local minimum.

To ensure the correct implementation of this concept, a repository to store all explorer particles and the first conqueror particles was created avoiding that the explorer particles visit regions close to those already created. This repository is mathematically defined by:

$$MC(t) = \frac{\sum_{x \in \mathcal{R}(t)} x}{\text{card}(\mathcal{R}(t))}, \quad (6)$$

where $\mathcal{R}(t)$ is the repository in the iteration t , $\text{card}(\mathcal{R}(t))$ is the number of elements of $\mathcal{R}(t)$ and $MC(t)$ is the point that summarizes the behavior of the system in the iteration t . Since it was created to be analogous to a center of mass of an object the $MC(t)$ is defined as a centre of mass.

Also, it is necessary a new velocity equation that can rule the new explorer behavior in this modification, so the Eq. (7) was defined in order to change the particle dependency from the old global best position to the new centre of mass,

$$v_i(t+1) = w \delta \cdot v_i(t) + c_1 \phi \cdot (p_i - x_i(t)) + c_3 \rho \cdot \exp\left(-\alpha \cdot \frac{|x_i(t) - MC(t)|}{x_{max} - x_{min}}\right) \cdot (x_i(t) - MC(t)), \quad (7)$$

where x_{max} , x_{min} are vectors of dimension D that represent the boundaries of the search space and δ , ϕ and ρ are random vectors like in Eq. (5). The quotient is given by Eq. (8) and should be carried out componentwise.

$$\frac{x_i(t) - MC(t)}{x_{max} - x_{min}} \quad (8)$$

Besides, a set of Neural Networks (NN) were trained and coupled with the novelty swarm algorithm as an additional step in order to enhance the convergence. A specific NN for each output parameter (NO_x , soot and efficiency) was trained every 30 iterations of the algorithm using all inputs (geometrical inputs, injection and air management systems inputs) and outputs of all cases.

The optimization flow chart can be seen in the Fig. 4.

3.5. Tools

In order to perform many simulations automatically in the optimization process several tools were used. The first one is a tool to generate the combustion chamber geometry through Bezier polynomial curves [34] using six different parameters. Each one of these six geometry parameters are independent, dimensionless and have their own range in

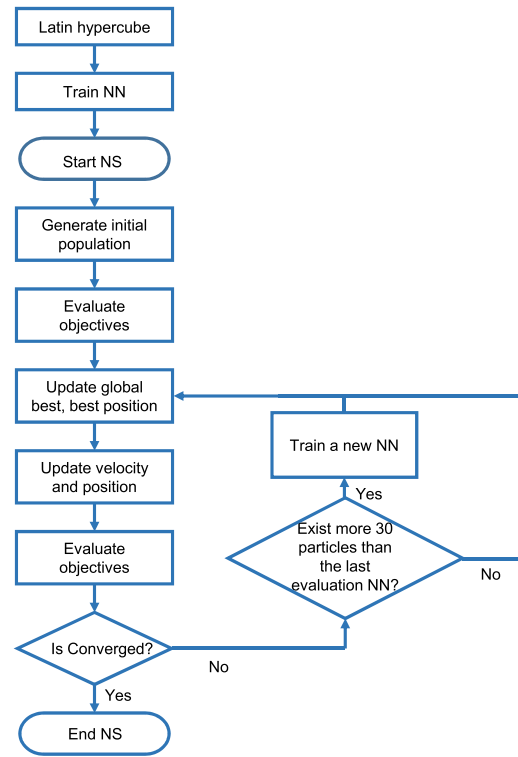


Fig. 4. Flow chart of optimization process.

different parts of the geometry. Fig. 5 shows different examples of bowl geometries that are obtained by this method. Changes in the bowl geometry have a direct influence on the volume of the combustion chamber, then the squish height was adjusted in order to maintain the CR in 16, as in the original engine.

In the next step, after the bowl profile geometry is configured, it is necessary to generate the mesh that is used to perform the simulations. This process is performed by a python code that generates the mesh automatically using the dynamic mesh layering technique developed by Lucchini et al. in [19] and, this method keeps fixed the cells in the spray region and move the cells close to the piston bowl. This tool divides the domain in several regions or blocks that are defined by control points. The position of these control points is adapted to each bowl profile in order to obtain a mesh that fulfils the orthogonality and cell skewness criteria. Moreover, it configures the cell orientation near the nozzle exit accordingly with the included spray angle of the spray, so the cells are oriented with the injection plume. An example of the control points and block definition is presented in Fig. 6. Finally, the mesh sector is constructed as a function on the number of holes of the injector, since each simulation is carried out for a region of the combustion chamber with only one spray, based on the axy-symmetric assumption that was mentioned before.

The rate of injection (ROI) profile was defined using a virtual injector model (VIM), which is an in-house code that builds a mass flow rate curve from a combination of various injection parameters [35,22]. In this work the parameters used are the total mass fuel injected in one cycle, injection pressure and the number of orifices of the injector, which affects the hole diameter. Since the nozzle permeability was kept constant, it was necessary to correct the nozzle diameter for all cases and this property defines the nozzle flow capacity and the injection duration. The total mass per cylinder is considered constant for all the cases and the other two parameters are variables of the optimization process. The VIM code assumes that the flow is incompressible across the nozzle holes and applies the equations of continuity and Bernoulli between the inlet and outlet of the orifices, providing a ROI based on a trapezoidal form as can be observed in the Fig. 7. The model is also calibrated for the OME

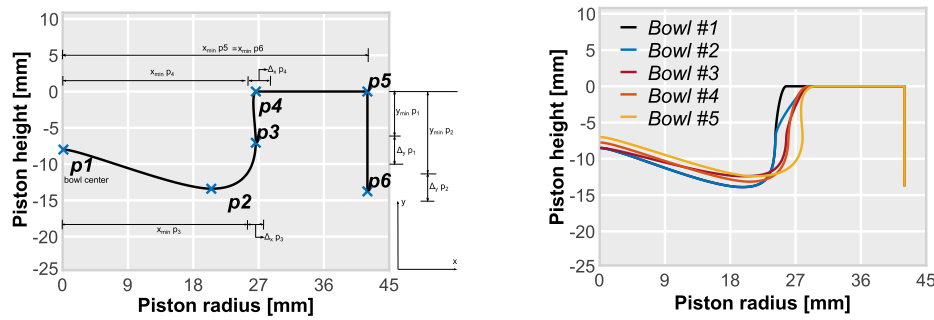


Fig. 5. Parameters definition for Bezier curves (Left-hand side) and examples of bowls that can be obtained for combustion chamber geometry (Right-hand side).

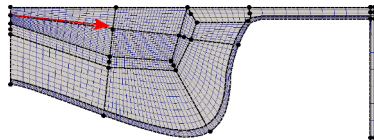


Fig. 6. Mesh generator: control points and block definition.

fuel used in this study, adjusting the ROI to compensate the LHV and the density as was indicated in Section 2.

After the generation and the simulation of each case, it is post-processed for extracting the values of efficiency, NO_x and soot emissions, among others. The performance of the combustion system is evaluated by means of a merit function that considers simultaneously an increase in efficiency and a reduction of pollutant emissions, compared to the reference case. At the same time, the merit function penalizes the cases that exceed the baseline NO_x value and corroborates that the soot levels are below the diesel case, which is expected due to the low sooting nature of the fuel. To meet these requirements the merit function was formulated considering the importance of each output from the simulation and the global function is composed by all the sub-functions of each output. Those functions are detailed in Eqs. (9)–(12).

$$f_1(NO_x) = \left. \begin{cases} \frac{NO_{x,CFD}}{NO_{x,lim}} & \text{if } NO_{x,CFD} < NO_{x,lim} \\ \frac{NO_{x,CFD}}{NO_{x,lim}} + 100 \cdot (NO_{x,CFD} - NO_{x,lim})^2 & \text{if } NO_{x,CFD} \geq NO_{x,lim} \end{cases} \right\} \quad (9)$$

$$f_2(soot) = \left. \begin{cases} \frac{-\log(soot_{CFD})}{\log(soot_{lim})} & \text{if } soot_{CFD} < soot_{lim} \\ \frac{-\log(soot_{CFD})}{\log(soot_{lim})} + 1000000 \cdot (\log(soot_{CFD}) - \log(soot_{lim}))^2 & \text{if } soot_{CFD} \geq soot_{lim} \end{cases} \right\} \quad (10)$$

$$f_3(eff) = \left. \begin{cases} \frac{-\log(ef_{CFD})}{-\log(ef_{lim})} & \text{if } ef_{CFD} > ef_{lim} \\ \frac{-\log(ef_{CFD})}{-\log(ef_{lim})} + 100 \cdot (\log(ef_{CFD}) - \log(ef_{lim}))^2 & \text{if } ef_{CFD} \leq ef_{lim} \end{cases} \right\} \quad (11)$$

$$OF = f_1(NO_x) \cdot coef_{NO_x} + f_2(soot) \cdot coef_{soot} + f_3(ef) \cdot coef_{ef} \quad (12)$$

where $NO_{x,CFD}$, $soot_{CFD}$ and ef_{CFD} are the values obtained in the CFD simulation, and the $NO_{x,lim}$, $soot_{lim}$ and ef_{lim} refer to the outputs of the reference engine. Finally, $coef_{NO_x}$, $coef_{soot}$ and $coef_{ef}$ are coefficients used to adjust the equation according to the order of importance of the parameters in the optimization.

As the main objective is to increase the efficiency of the engine at the same time as it reduces its NO_x and soot emissions, the values of the coefficients used are: $coef_{NO_x} = 0.05$, $coef_{soot} = 0.001$ and $coef_{ef} = 1$.

Aiming to optimize the combustion chamber, twelve relevant parameters of the combustion system were chosen, where six of them are related to the geometry definition of the bowl, three of them define the injection system (number of injection nozzle holes, spray angle and injection pressure), and the other three to the in-cylinder gas conditions (swirl number at IVC, EGR, IVC pressure). The range of those inputs variables are shown in Table 6.

4. Results and discussion

In this section, the results obtained from the optimization process are presented and discussed. First, the convergence of the PSO-NS algorithm is shown and trends of the output parameters are analyzed. Then, the results of the optimized combustion system are compared against the experimental and baseline case for a better understanding of this new combustion system.

4.1. Optimization results

The initial step of the results analysis was the algorithm convergence verification. The analysis of the algorithm convergence is performed through the mathematical analysis of the objective function value for all

particles calculated from the CFD data simulation. Fig. 8 shows how the PSO-NS algorithm consistently decreases the minimum objective function value, converging towards a minimum value. The best particle would be the one with the minimum value of the objective function until that iteration. At the beginning of the procedure it is observed how the objective function suddenly decreases, due to the PSO-NS rapid convergence capacity, until case number 780 where it reaches the minimum value of the objective function.

To obtain the location of the particle that provides the best solution in the explored range, the efficiency and NO_x were compared in a Pareto front that is presented in Fig. 9. In this plot all the simulated particles

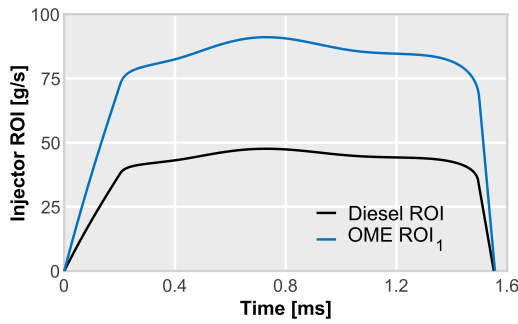


Fig. 7. Virtual injector model: comparison between the rate of injection profile between conventional fuel and OME.

Table 6

Parameters and ranges considered in the optimization process.

Parameter	Range
Geometrical parameter 1 [-]	[-0.5, 1.0]
Geometrical parameter 2 [-]	[-1.0, 1.25]
Geometrical parameter 3 [-]	[-1.0, 1.0]
Geometrical parameter 4 [-]	[0.0, 1.0]
Geometrical parameter 5 [-]	[-1.4, 0.1]
Geometrical parameter 6 [-]	[-0.5, 1.0]
Number of injector nozzles [-]	[4,12]
Spray angle [°]	[155, 170]
Swirl number at IVC [-]	[1.0, 3.0]
Injection pressure [bar]	[1500, 2000]
EGR [%]	[0, 30]
IVC pressure [%]	[0, 30]

were used to show the trade-off between both parameters to optimize. The optimum value is shown on the figure as a red dot. Moreover, from Fig. 9 it is possible to find particles that provide better results than the optimized particle for each output in separately, sacrificing part of the efficiency it is possible to obtain better NO_x emissions and the opposite is also possible, sacrificing fractions of NO_x it is possible to obtain better efficiencies.

Based on the results of the objective function, the optimized configuration was compared with the reference diesel case that was used to reproduce the experimental conditions. In Fig. 10, the differences between bowl geometry and spray angle can be observed. Regarding the optimized geometry, a re-entrant bowl shape is used instead of a step-bowl profile. One of the purposes of the step-bowl geometry is to deflect the spray towards the cylinder head to prevent an excess of spray-wall impingement on the liner, avoiding soot-in-oil generation. Since OME is a low sooting fuel, this deflection is not required because there is

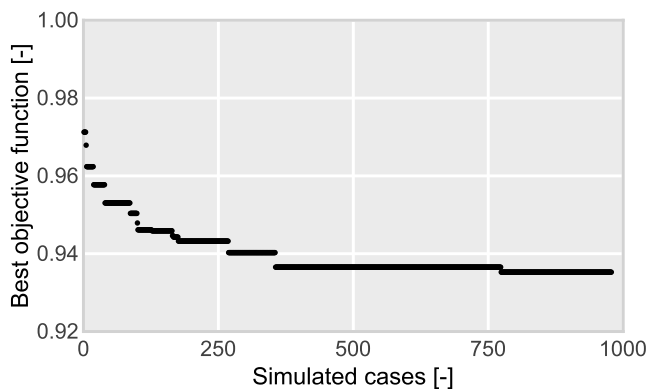


Fig. 8. Objective function convergence.

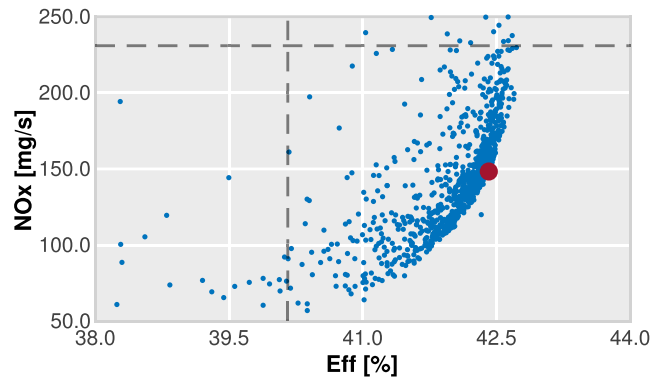


Fig. 9. Pareto front of NO_x emissions vs. efficiency of the engine. The blue dots are the results of all cases simulated in the optimization process and the red dot is the optimized case. (For interpretation of the references to color in this figure legend, the reader is referred to the web version of this article.)

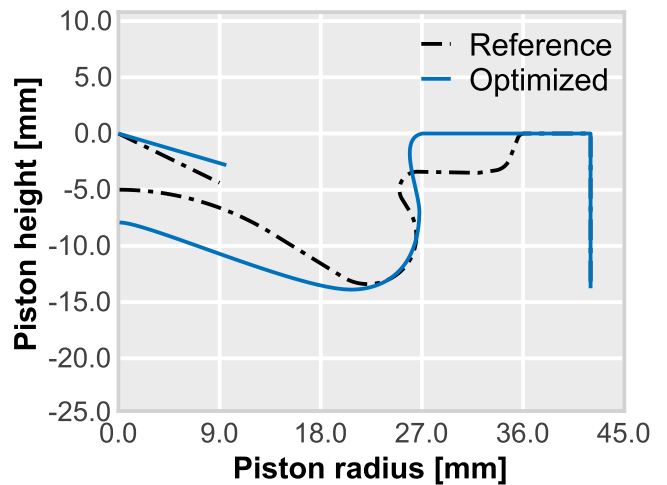


Fig. 10. Bowl profile comparison between reference diesel case and optimized OME case.

Table 7

Inputs comparison between baseline OME and optimized OME cases.

	OME Baseline case	Optimized case
Number of holes [-]	10	9
Spray angle [deg]	154	164
Swirl number [-]	2.00	2.83
Injection pressure [bar]	1800	2216
EGR rate [%]	0	17.3
IVC pressure [bar]	3.89	4.04

negligible risk for generating soot particles near the liner region. This new geometry may also decrease the heat transfer through the cylinder head, preserving the mechanical integrity of this component and contributing to a better efficiency. Furthermore, the spray angle is adjusted with the bowl piston shape.

Additionally, Table 7 lists the complete parameters of the combustion system for both cases. The number of injector nozzle holes are decreased to 9 which leads to larger orifice diameters in order to maintain the same nozzle area. The spray angle is 10 degrees greater which enables the spray to better adjust to the geometry of the bowl. The injection pressure is higher than the reference value, enhancing the mixing rate due to a higher spray momentum, improved atomization and faster evaporation. Apart from that, the optimized case has an EGR rate of 17.3% and an IVC pressure slightly higher than the initial

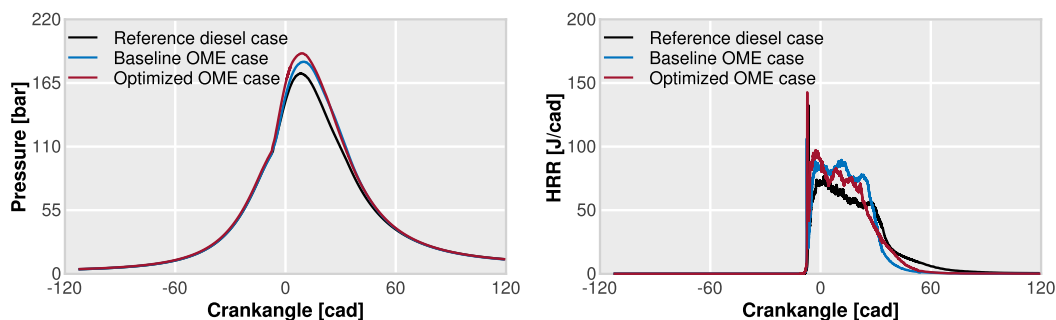


Fig. 11. Comparison of in-cylinder pressure and rate of heat release between reference diesel case, baseline OME case and optimized OME case.

baseline configuration.

In Fig. 11, the in-cylinder pressure and rate of heat release comparison between the reference diesel case, baseline OME case and the optimized OME case are shown. The baseline OME case has the same configuration of the diesel reference case while using OME as the fuel. The optimized OME case obtained from the PSO-NS using OME as fuel is presented in this figure as well. By examining the pressure trace, it is possible to note the differences between all cases. The differences related to the maximum peak of pressure obtained for the cases using OME can be a result of the greater amount of fuel needed to compensate the lower LHV of the OME. A combination of the higher injection pressure together with the larger nozzle holes leads to a faster energy delivery causing a higher cylinder pressure level.

The heat release rate of the optimized case with OME presents a higher burn rate compared with the reference diesel case, showing a higher peak of the premixed phase, and for the rest of the combustion duration. Furthermore, the heat release rate is slightly shortened since the injection pressure is higher, decreasing the duration of the injection event to ensure that the same amount of fuel is injected for all cases. The high levels of heat release combined with a shorter duration improves the combustion performance, and leads to thermodynamic advantages, such as improved combustion efficiency and a thermodynamic cycle closer to the ideal one. The enhanced combustion process is related to a better distribution of the mixture within the system as is discussed later on.

The results obtained from the optimized case are shown in Table 8 where they are compared against the reference diesel case and the OME baseline case. Comparing the reference diesel against the optimized case, a combustion system was obtained that produces 35.7% less NO_x , 2.2% higher efficiency and a great reduction of soot due to the non-sooting characteristics of OME. Even though the baseline OME case has a higher efficiency than the other two cases, the NO_x value is unacceptable, therefore it is necessary to sacrifice part of the efficiency in order to reduce the NO_x level. In general, the combination of a higher injection pressure with higher swirl ratio contributes to better atomization and evaporation and shortens combustion duration. With the new configuration there is more space between the sprays avoiding spray interaction resulting in NO_x reduction with better efficiency. The great NO_x reduction can be explained principally by the EGR rate of the optimized case. The EGR reduces the local temperature near the flame regions leading to a lower NO_x concentration.

The temporal evolution of the NO_x emission as the combustion

progresses is shown in Fig. 12 (right-hand side). Compared to the reference diesel case, the NO_x formation in the baseline OME case has the highest values, and correlates well with the maximum mean temperature in the cylinder between 12 and 40 CAD, as can be seen on the left-hand side of the same figure. This increment can be attributed to an excess of local temperature above 1800 K promoting an exponential NO_x formation as previously demonstrated by Turns in [36] and Drake in [37]. Regarding the optimized case the mean temperature overlaps that of the OME baseline during the premixed phase of the combustion. However, during the later stages, the temperature of the optimized case is lower due to the EGR rate used that provides an increase in the heat capacity of the mixture acting as NO_x controller. The vertical dashed lines in Fig. 12 represent four crankangles (0, 12, 40, 27 and 60) selected for comparing the temperature distribution in the combustion chamber for the analyzed cases.

Fig. 13 shows the temperature contours for the diesel reference diesel case, the baseline OME case (with the same geometry of the initial diesel engine) using OME as fuel and the best case obtained from the optimization. Mainly, the changes in the bowl profile increases the distance between the nozzle hole outlet and the walls of the piston bowl, which is in agreement with previous studies [17,14], that presented larger combustion chambers when oxygenated fuels are used due to the longer mixing lengths for those fuel sprays. In addition, the optimized case exhibits a faster jet penetration, which occurs due to bigger orifice diameters and higher injection pressure. The included spray angle that matches the bowl profile is wider than the reference case, directing the spray towards the inferior side of the re-entrant edge of the profile when the piston is at top dead center, as can be seen from the first image at the bottom left side. The onset of combustion appears to mainly consume the air present in the piston bowl. As the piston moves towards the bottom dead center, the spray impacts on the edge of the bowl, splits, and then finds the air available in the outer regions of the bowl increasing the mixing rate and improve the distribution of the flame inside the combustion chamber. Moreover, the optimized case has a higher swirl number that could produce an overlap of the plumes promoting unfavorable combustion conditions, however this inconvenience is surpassed by using a nozzle with one less hole compared to the initial configuration. The use of the 9 hole configuration restricts the plume-to-plume interaction and avoids the formation of fuel-rich zones. Therefore, in the last stage of the combustion a more homogeneous temperature distribution is found leading to a better performance of the system, corroborating the behaviour previously shown in Fig. 12.

Table 8

NO_x , soot and efficiency comparison between reference, baseline and optimized cases.

Case	NO_x [mg/s]	Soot [mg/s]	Efficiency [%]
Reference case	230.95	0.355	40.2
Baseline OME case	773.60	<0.0001	43.0
Optimized OME case	148.32	<0.0001	42.4

4.2. Parametric study for sensitivity analysis

This section presents the results obtained from a parametric study realized using machine learning methods. The PSO-NS methodology enabled to obtain an optimum design in a reasonable number of simulations and also generated a large data set with useful information about the combustion system. A neural network model (NN) was trained from the data generated by the optimization process. The model is a

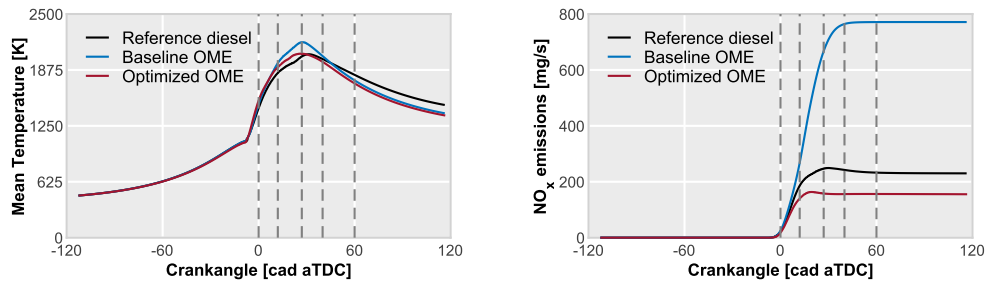


Fig. 12. In-cylinder mean temperature and NO_x emissions, a comparison between the reference diesel case, baseline OME case and the optimized OME case.

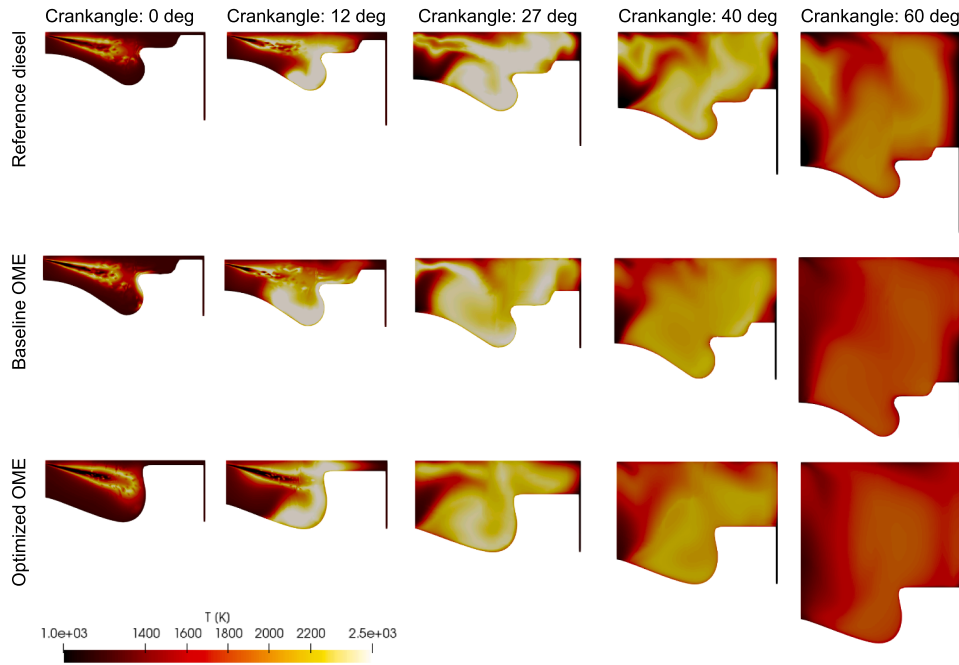


Fig. 13. In-cylinder temperature contours comparison between the reference diesel case, baseline OME case and the optimized OME case.

mathematical approach that acts as a surrogate model for the CFD simulations. Two different NN were trained from the data generated during the optimization process where, the first one predicts the engine efficiency behavior and the second one reproduces the NO_x emissions behavior. A NN model for soot emissions was neglected since the values obtained during the optimization process were imperceptible (as expected due to the low-sooting capability of this fuel). The NN used in this work was developed in Python [38] using packages as Numpy together with the open-source libraries Keras [39]. A kernel L2 regularization was used for all hidden layers to improve the accuracy of the prediction during the training phase [40]. Adam optimization algorithm [41] was

used with the training algorithm for updating the NN weights. The maximum number of iterations of the algorithm was set to 500. In order to choose the best set of parameters for the NN, a KerasRegressor has been implemented. Also, a k-fold cross validation was used, which consists of an iterative division of the data used in the train process and another data for the testing. The NN was trained with 67% of the total data (that is two thirds of the 950 simulated cases) and tested with the 33% of the remaining data, selected randomly.

In order to evaluate the quality of the prediction both NNs were tested using the optimum case configuration, predicting the outputs of this case and comparing them against the results obtained from the CFD

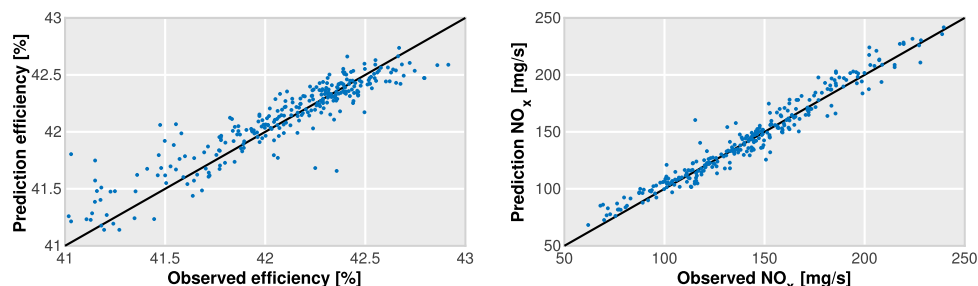


Fig. 14. NN-based predicted vs CFD observed. The left-hand side plot: efficiency regression. The right-hand side plot: NO_x prediction.

simulation. The predictions of efficiency and NO_x emissions resulted in 42.4% (42.415) and 155.67 mg/s respectively for the NN compared to the efficiency and NO_x emissions from the CFD case of 42.4% (42.412) and 148.32 mg/s, which means a difference of 0.008% for the efficiency and 4.96% for NO_x emissions. Moreover, Fig. 14 shows the predicted values obtained from the NN regression vs the CFD results for efficiency (left plot) and for the NO_x values (right plot). In general, the prediction of the NO_x concentration is more precise than the prediction of the efficiency. This behaviour was observed by other authors before. For instance, Owoyele et al. [42] also found that the NN predictions are more accurate for the NO_x results than for other variables as ISFC or soot emissions. Overall, the NN reproduces the trend of the efficiency and NO_x emissions quite well with a reasonable accuracy level.

Aiming at a better understanding of the combustion system a sensitivity analysis was performed based on the trained NN. For this part of the study, the piston bowl design was kept the same while other parameters were varied, such as: number of holes of the injector, the spray angle, the injection pressure, the EGR rate and the IVC pressure. The goal was to evaluate the behavior of the efficiency and NO_x emissions of the optimum geometry with different parameters focusing on the engine settings and operation. The proposed parameters with their respective range for this sensitivity analysis are presented in Table 9.

To isolate the effect of each parameter, a matrix of cases was created varying just one parameter each time, it means the cases used to the study influence of the number of holes in the combustion chamber have the same configuration than the optimized, except to the number of holes. The same procedure was applied to the others parameters that were tested in this analysis.

Fig. 15 shows all the results obtained from this parametric study for efficiency and NO_x emissions. From a general perspective, the parameters that have a considerable influence are the injection pressure and the EGR rate on NO_x emissions and efficiency, meanwhile, the nozzle configuration and the IVC pressure have a lower effect. The effect of nozzle hole number on NO_x and efficiency is shown on Fig. 15 and it is possible to note that a maximum value was obtained for the efficiency when the injector has 9 holes. Hence, a compromise should be taken since reducing the number of holes would lead to bigger droplets being injected due to the larger hole diameters. This in turn worsens the atomization and mixing process between the fuel and air. On the contrary, increasing the number of holes would cause a significant plume-to-plume interaction which negatively impacts the combustion process. This could also lead to higher number of rich zones and a reduced efficiency having a similar behavior to that presented by Mohiuddin in [43]. Regarding the NO_x emissions trend, increasing the number of holes while maintaining the same operating conditions results in a smaller droplet size of fuel which means a better atomized spray enhancing the mixture, and leading to a reduction of emissions.

Concerning the included spray angle, it must be noted that when the bowl design is decided the injector configuration is usually kept constant. Nevertheless, small variations of the spray angle have very little consequences on the efficiency and NO_x emissions. In addition, the impact of the IVC pressure on both efficiency and NO_x emissions is negligible, as can be seen in the figures where the plot is constant. Regarding the EGR rate and the injection pressure, it is possible to observe that these parameters have a big influence on efficiency and

NO_x emissions in the range evaluated. When the EGR rate is increased, the burning rate of the non-premixed combustion phase is increased, leading to a reduction in efficiency and a reduction in NO_x emissions. This effect was also observed in literature in some works presented by Shi and Reitz in [44], Benajes in [34] and Mohiuddin [43]. The last parameter evaluated was the injection pressure that shows a substantial influence on the efficiency and NO_x emissions. The injection pressure increases the liquid phase momentum and the evaporation. When the injection pressure is increased a better mixing is expected, which promotes a better combustion and leads to a higher temperature inside the combustion chamber. On one hand, the higher temperature improves the efficiency, and on the other hand, it promotes the formation of NO_x. Based on this study, it is possible to predict the behavior of the engine and to further evaluate settings and configurations that can be used on an engine test bench.

Finally, a variability study is shown in Table 10 where the variations for each parameter are calculated aiming to obtain an analytical representation of the results showed in Fig. 15. From Table 10 it is possible to observe that the appropriate set of parameters could result in an improvement of efficiency up to 1.2%. For what concerns the NO_x emissions, the correct set of the injection pressure and EGR can reduce the emissions in the engine by 60%. An interesting point is that these two parameters, injection pressure and EGR rate, can be changed directly during engine operation which allows a quick adjustment in the set of parameters in order to obtain better NO_x emissions. The information this part of the study offers is valid in the case the system is manufactured, a facilitates a better understanding of its sensitivity to the parameters, and could be useful even for guiding engine calibration strategies.

5. Conclusion

In this study, a methodology for CFD-guided optimization of the combustion system of an engine using OME as a fuel was performed. This methodology was based on the combination of PSO-NS algorithm and CFD modeling. This study aims to improve the efficiency and to reduce the NO_x emissions of a CI engine through the optimization of the piston bowl geometry, injection and air-management systems.

An initial validation against available experimental data of an engine fuelled with conventional diesel was performed. With the validated model the fuel was replaced by OME and the mass of fuel was corrected in order to maintain the same amount of energy available in the cycle.

Different tools were used to create the CFD model for each case. The first tool creates the piston bowl profile from the geometrical parameters defined by the optimization algorithm. Another tool builds the mesh that is used in the simulations. The third tool generates the specific rate of injection of each case. Furthermore, a routine couples the optimization algorithm and all the tools used to configure the CFD case, meaning that, the entire optimization process was performed automatically.

A PSO algorithm adapted with the NS methodology was used for the optimization process. Thirteen inputs were used for this optimization: 6 parameters for defining the piston bowl geometry, 3 parameters for the injection system description (number of holes of the injector, included spray angle, injection and injection pressure). The air-management system is defined by the swirl number, the pressure at IVC and the EGR rate. The evaluation of each simulation case was made by the evaluation of the objective function, which quantifies the set of inputs in value calculated using the values of the efficiency and NO_x emissions obtained from the simulations for each case.

During the optimization process around 1000 simulations were performed in order to obtain an optimized configuration. The injection system that matches the best case has one less nozzle orifice, a wider spray angle that better suits the piston bowl geometry, and a higher injection pressure. Concerning the air-management system, the optimum configuration increases the EGR rate considerably, and in a smaller proportion the swirl number and the IVC pressure. With this new

Table 9
Parameters used to study the optimum combustion chamber behavior.

Parameter	Range
Number of holes [-]	[8, 10]
Spray angle [def]	[161, 165]
Injection pressure [bar]	[2000, 2400]
EGR rate [%]	[14, 20]
IVC pressure [bar]	[3.9, 4.1]

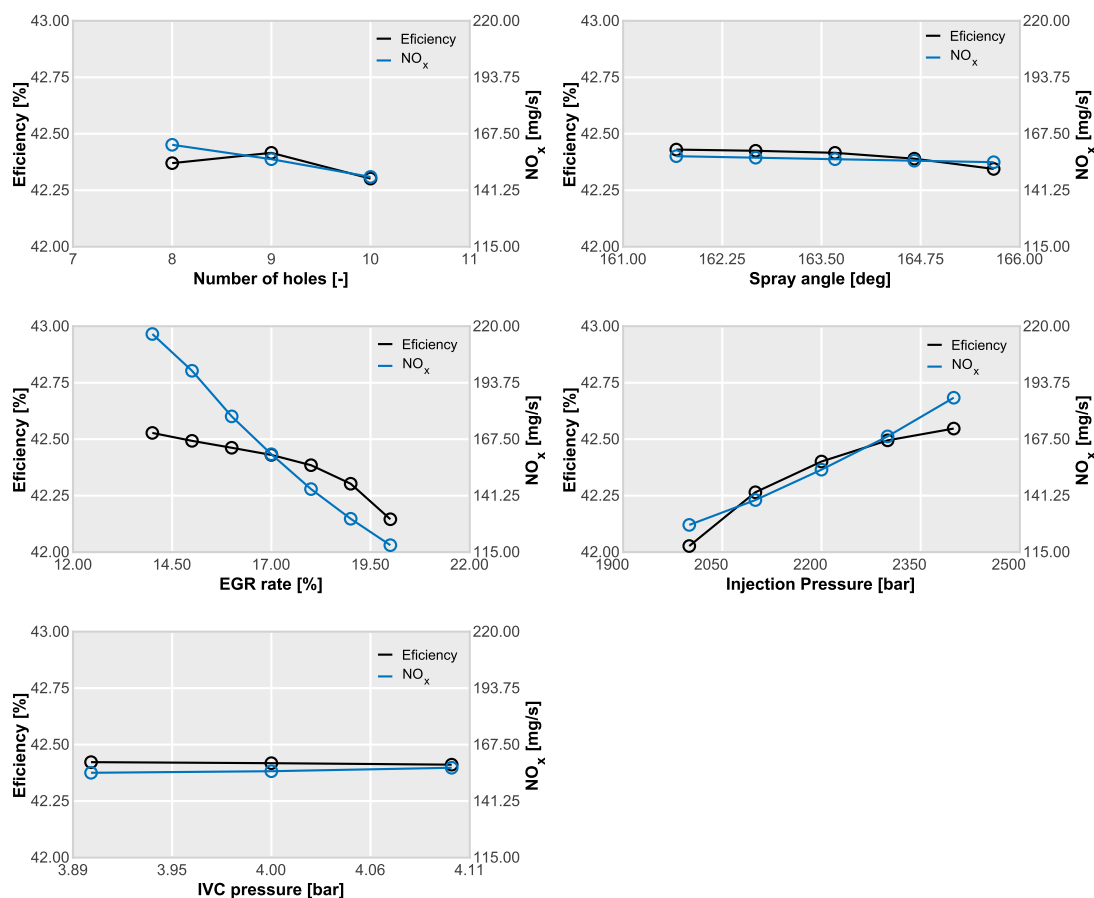


Fig. 15. Efficiency and NO_x results from the parametric study using machine learning tools.

Table 10

Variability of each parameter based on the optimum value.

	Efficiency variation [%]	NO_x variation [%]
Number of holes [-]	0.27	9.59
Spray angle [deg]	0.20	1.79
Injection pressure [bar]	1.23	37.99
EGR rate [%]	0.90	63.08
IVC pressure [bar]	0.03	1.49

configuration it was possible obtain a better engine efficiency, around 2.2% higher with a great reduction of the NO_x emissions, around 35.7% in comparison with the reference diesel engine.

Based on the optimized case a parametric study using NN was performed to evaluate how each parameter affects the efficiency and NO_x emissions. The optimized geometry was kept constant whereas the number of holes, spray angle, injection pressure, EGR rate and IVC pressure varied in a range close to the optimized design. The objective of this part of the study was to better understand the combustion chamber system and the influence of each parameter on efficiency and emissions. It was obtained that the number of holes, spray angle and IVC pressure factors have little impact on the engine efficiency. However, the injection pressure can provide a significant increase, up to 1.2% more efficiency followed by the EGR rate. For the case of NO_x emissions, the EGR rate shows a great influence on this emission value in the order of 63% followed by the injection pressure with 38% of influence.

To summarize, the optimization process combined with CFD simulations can help to develop a specific combustion system for an engine that aims to use OME as a fuel providing good results in terms of efficiency and a NO_x emissions.

CRedit authorship contribution statement

Ricardo Novella: Supervision, Project administration, Resources, Writing - review & editing. **Gabriela Bracho:** Conceptualization, Methodology, Formal analysis, Investigation, Writing - review & editing. **Josep Gomez-Soriano:** Writing - review & editing, Formal analysis. **Cássio S. Fernandes:** Conceptualization, Methodology, Formal analysis, Investigation, Writing - original draft. **Tommaso Lucchini:** Conceptualization, Writing - review & editing.

Declaration of Competing Interest

The authors declare that they have no known competing financial interests or personal relationships that could have appeared to influence the work reported in this paper.

Acknowledgements

The work has been partially supported by the Spanish Ministerio de Economía, Industria y Competitividad through Grant No TRA2017-89139-C2-1-R "Desarrollo de modelos de combustión y emisiones HPC para el análisis de sistemas de transporte sostenibles"

The author C. S. Fernandes thanks the Universitat Politècnica de Valencia for his predoctoral contract (FPI-2019-S2-20-555), which is included within the framework of Programa de Apoyo para la Investigación y Desarrollo (PAID).

Appendix A. Supplementary data

Supplementary data associated with this article can be found, in the online version, at <https://doi.org/10.1016/j.fuel.2021.121580>.

References

- [1] Intergovernmental Panel on Climate Change. Climate Change 2014 Mitigation of Climate Change; 2014. doi:10.1017/cbo9781107415416.
- [2] G. Valentino, L. Allocca, L. Marchitto, PIV investigation of high swirl flow on spray structure and its effect on emissions in a diesel-like environment. SAE 2011 World Congress and Exhibition doi:10.4271/2011-01-1286.
- [3] Iannuzzi SE, Barro C, Boulouchos K, Burger J. Combustion behavior and soot formation/oxidation of oxygenated fuels in a cylindrical constant volume chamber. Fuel 2016;167:49–59. <https://doi.org/10.1016/j.fuel.2015.11.060>.
- [4] Lautenschütz L, Oestreich D, Seidenspinner P, Arnold U, Dinjus E, Sauer J. Physico-chemical properties and fuel characteristics of oxymethylene dialkyl ethers. Fuel 2016;173:129–37. <https://doi.org/10.1016/j.fuel.2016.01.060>.
- [5] Liu H, Wang Z, Zhang J, Wang J, Shuai S. Study on combustion and emission characteristics of Polyoxymethylene Dimethyl Ethers/diesel blends in light-duty and heavy-duty diesel engines. Appl Energy 2017;185:1393–402. <https://doi.org/10.1016/j.apenergy.2015.10.183>.
- [6] Omari A, Heuser B, Pischinger S. Potential of oxymethylenether-diesel blends for ultra-low emission engines. Fuel 2017;209(May):232–7. <https://doi.org/10.1016/j.fuel.2017.07.107>.
- [7] Y.R. Tan, M.L. Botero, Y. Sheng, J.A. Dreyer, R. Xu, W. Yang, M. Kraft, Sooting characteristics of polyoxymethylene dimethyl ether blends with diesel in a diffusion flame. Fuel 2018;224(November 2017):499–506. doi:10.1016/j.fuel.2018.03.051.
- [8] F. Ferraro, C. Russo, R. Schmitz, C. Hasse, M. Sirignano, Experimental and numerical study on the effect of oxymethylene ether-3 (OME3) on soot particle formation. Fuel (P1):119353. doi:10.1016/j.fuel.2020.119353.
- [9] Burger J, Siegert M, Ströfer E, Hasse H. Poly(oxymethylene) dimethyl ethers as components of tailored diesel fuel: Properties, synthesis and purification concepts. Fuel 2010;89(11):3315–9. <https://doi.org/10.1016/j.fuel.2010.05.014>.
- [10] Burger J, Ströfer E, Hasse H. Production process for diesel fuel components poly(oxymethylene) dimethyl ethers from methane-based products by hierarchical optimization with varying model depth. Chem Eng Res Des 2013;91(12):2648–62. <https://doi.org/10.1016/j.cherd.2013.05.023>.
- [11] Härtl M, Seidenspinner P, Jacob E, Wachtmeister G. Oxygenate screening on a heavy-duty diesel engine and emission characteristics of highly oxygenated oxymethylene ether fuel OME1. Fuel 2015;153:328–35. <https://doi.org/10.1016/j.fuel.2015.03.012>.
- [12] Deutz S, Bongartz D, Heuser B, Kätelhön A, Schulze Langenhorst L, Omari A, et al. Cleaner production of cleaner fuels: Wind-to-wheel-environmental assessment of CO₂-based oxymethylene ether as a drop-in fuel. Energy Environ Sci 2018;11(2):331–43. doi:10.1039/c7ee01657c.
- [13] Pélerin D, Gaukel K, Härtl M, Jacob E, Wachtmeister G. Potentials to simplify the engine system using the alternative diesel fuels oxymethylene ether OME1 and OME3-6 on a heavy-duty engine. Fuel January 2019;259. <https://doi.org/10.1016/j.fuel.2019.116231>.
- [14] Gaukel K, Dworschak P, Pélerin D, Härtl M, Wachtmeister G. Combustion process optimization for oxymethylene ether fuels in a heavy-duty application 2019: 351–67. https://doi.org/10.1007/978-3-658-26528-1_21.
- [15] Broatch A, Novella R, Gomez-Soriano J, Pal P, Som S. Numerical methodology for optimization of compression-ignited engines considering combustion noise control. SAE Int J Engines 2018;11(6):625–42. <https://doi.org/10.4271/2018-01-0193>.
- [16] Bertram AM, Zhang Q, Kong SC. A novel particle swarm and genetic algorithm hybrid method for diesel engine performance optimization. Int J Engine Res 2016;17(7):732–47. <https://doi.org/10.1177/1468087415611031>.
- [17] Zübel M, Ottenwälder T, Heuser B, Pischinger S. Combustion system optimization for dimethyl ether using a genetic algorithm. Int J Engine Res 2021;22(1):22–38. <https://doi.org/10.1177/1468087419851577>.
- [18] Montenegro G, Onorati A, Piscaglia F, D'Errico G. Integrated 1d-multid fluid dynamic models for the simulation of ice intake and exhaust systems. SAE Techn Pap Ser 2007;1:776–90. <https://doi.org/10.4271/2007-01-0495>.
- [19] Lucchini T, D'Errico G, Jasak H, Tukovic Z. Automatic mesh motion with topological changes for engine simulation. SAE Techn Pap Ser 2007;1:1–20. <https://doi.org/10.4271/2007-01-0170>.
- [20] Ismail H, Ng H, Gan S, Lucchini T. Approach for the modeling of reacting biodiesel fuel spray using openfoam. SAE Techn Pap Ser 2014;1:1–9. <https://doi.org/10.4271/2014-01-2565>.
- [21] D'Errico G, Lucchini T, Hardy G, Tap F, Ramaekers G. Combustion modeling in heavy duty diesel engines using detailed chemistry and turbulence-chemistry interaction. SAE Techn Pap Ser 2015;1:1–14. <https://doi.org/10.4271/2015-01-0375>.
- [22] Payri R, Gimeno J, Novella R, Bracho G. On the rate of injection modeling applied to direct injection compression ignition engines. Int J Engine Res 2016;17(10):1015–30. <https://doi.org/10.1177/1468087416636281>.
- [23] Ismail HM, Ng HK, Gan S, Lucchini T, Onorati A. Development of a reduced biodiesel combustion kinetics mechanism for cfd modelling of a light-duty diesel engine. Fuel 2013;106:388–400. doi:https://doi.org/10.1016/j.fuel.2012.10.015.
- [24] Ismail HM, Ng HK, Cheng X, Gan S, Lucchini T, D'Errico G. Development of thermophysical and transport properties for the cfd simulations of in-cylinder biodiesel spray combustion. Energy Fuels 2012;26(8):4857–70. <https://doi.org/10.1021/ef300862u>.
- [25] Yakhot V, Orszag SA. Renormalization-group analysis of turbulence 1986;57(14):1722–4.
- [26] D'Errico G, Lucchini T, Contino F, Jangi M, Bai XS. Comparison of well-mixed and multiple representative interactive flamelet approaches for diesel spray combustion modelling. Combust Theory Model (1):65–88. doi:10.1080/13647830.2013.860238.
- [27] D'Errico G, Lucchini T, Stagni A, Frassoldati A, Faravelli T, Ranzi E. Reduced kinetic mechanisms for diesel spray combustion simulations. SAE Techn Pap 6 (Cmc). doi:10.4271/2013-24-0014.
- [28] Lucchini T, Onorati A, Hardy G. CFD modelling of combustion in Heavy-Duty Diesel Engines 2014:1–15.
- [29] Zhou Q, Lucchini T, D'Errico G, Hardy G. SAE Technical Papers doi:10.4271/2019-24-0088.
- [30] Zhou Q, Lucchini T, D'Errico G, Hardy G, Lu X. Modeling heavy-duty diesel engines using tabulated kinetics in a wide range of operating conditions. Int J Engine Res 2021;22(4):1116–32. <https://doi.org/10.1177/1468087419896165>.
- [31] Benajes J, Olmeda P, Martín J, Carreño R. A new methodology for uncertainties characterization in combustion diagnosis and thermodynamic modelling. Appl Therm Eng 2014;71:389–99. <https://doi.org/10.1016/j.applthermaleng.2014.07.010>.
- [32] Kennedy J, Eberhart R. 47-Particle swarm optimization proceedings, In: IEEE International Conference, Proceedings of ICNN'95 – International conference on neural networks (1). p. 111–7.
- [33] Lehman J, Stanley KO. Exploiting open-endedness to solve problems through the search for novelty. Artificial Life - ALIFE.
- [34] Benajes J, Novella R, Pastor JM, Hernández-López A, Hasegawa M, Tsuji N, et al. Optimization of the combustion system of a medium duty direct injection diesel engine by combining CFD modeling with experimental validation. Energy Conv Manage 212–29 doi:10.1016/j.enconman.2015.12.010.
- [35] Payri R, Salvador FJ, Gimeno J, Bracho G. A new methodology for correcting the signal cumulative phenomenon on injection rate measurements. Exp Techniques 2008;32(1):46–9. <https://doi.org/10.1111/j.1747-1567.2007.00188.x>.
- [36] Turns SR. An introduction to combustion: concepts and applications, 3rd Ed., New York: McGraw-Hill, 2012, New York; 2012.
- [37] Drake MC, Blint RJ. Calculations of nox formation pathways in propagating laminar, high pressure premixed ch₄/air flames. Combust Sci Technol 1991;75 (4–6):261–85. <https://doi.org/10.1080/00102209108924092>.
- [38] Python programming language - <https://www.python.org>. URL: <https://www.python.org>.
- [39] Chollet F, et al. Keras; 2015. URL: <https://keras.io>.
- [40] Kukačka J, Golkov V, Cremers D. Regularization for deep learning: a taxonomy. 2017. p. 1–23. arXiv:1710.10686.
- [41] Kingma DP, Ba JL, Adam: A method for stochastic optimization. In: 3rd International conference on learning representations, ICLR 2015 - Conference track proceedings; 2015. p. 1–15 arXiv:1412.6980.
- [42] Owoyele O, Pal P, Torreira AV. An automated machine learning-genetic algorithm (AutoML-GA) framework with active learning for design optimization. In: ASME 2020 Internal Combustion Engine Division Fall Technical Conference, ICEF 2020 (November). doi:10.1115/ICEF2020-3000.
- [43] Mohiuddin K, Kwon H, Choi M, Park S. Experimental investigation on the effect of injector hole number on engine performance and particle number emissions in a light-duty diesel engine. Int J Engine Res doi:10.1177/1468087420934605.
- [44] Shi Y, Reitz RD. Optimization study of the effects of bowl geometry, spray targeting, and swirl ratio for a heavy-duty diesel engine operated at low and high load. Int J Engine Res 2008;9(4):325–46. <https://doi.org/10.1243/14680874JER00808>.